Minicircle-IFNγ Induces Antiproliferative and Antitumoral Effects in Human Nasopharyngeal Carcinoma

Jiangxue Wu,[1] Xia Xiao,[1] Peng Zhao,[1] Gang Xue,[2] Yinghui Zhu,[1] Xiaofeng Zhu,[1] Limin Zheng,[1] Yixin Zeng,[1] and Wenlin Huang[1,3]

Abstract

Purpose: The aims of this work were to investigate the antitumor effect of IFNγ gene transfer on human nasopharyngeal carcinoma (NPC) and to assess the potential of minicircle vector for antitumor gene therapy.

Experimental Design: We developed a recombinant minicircle vector carrying the human IFNγ gene and evaluated the effects of minicircle-mediated IFNγ gene transfer on NPC cell lines *in vitro* and on xenografts *in vivo*.

Results: Relative to p2ΦC31-IFNγ, minicircle-mediated IFNγ gene transfer *in vitro* resulted in 19- to 102-fold greater IFNγ expression levels in transfected cells (293, NIH 3T3, CNE-1, CNE-2, and C666-1) and inhibited the growth of CNE-1, CNE-2, and C666-1 cells more efficiently, reducing relative growth rates to 7.1 ± 1.6%, 2.7 ± 1.0%, and 6.1 ± 1.6%, respectively. Flow cytometry and caspase-3 activity assays suggested that the antiproliferative effects of IFNγ gene transfer on NPC cell lines could be attributed to G_0-G_1 arrest and apoptosis. Minicircle-mediated intratumoral IFNγ expression *in vivo* was 11 to 14 times higher than p2ΦC31-IFNγ in CNE-2- and C666-1-xenografted mice and lasted for 21 days. Compared with p2ΦC31-IFNγ treatment, minicircle-IFNγ treatment significantly increased survival and achieved inhibition rates of 77.5% and 83%, respectively.

Conclusions: Our data indicate that IFNγ gene transfer exerts antiproliferative effects on NPC cells *in vitro* and leads to a profound antitumor effect *in vivo*. Minicircle-IFNγ is more efficient than corresponding conventional plasmids due to its capability of mediating long-lasting high levels of IFNγ gene expression. Therefore, minicircle-mediated IFNγ gene transfer is a promising novel approach in the treatment of NPC.

IFNγ is capable of potently inhibiting growth in a number of tumor models (1–5). The antiproliferative actions were attributed to direct actions of IFNγ on tumor cells and indirect mechanisms, such as immunomodulation and antiangiogenesis (1–5). However, direct effects seem to be highly tissue and cell type specific (6, 7). Thus, elucidation of the mechanisms underlying the antitumor effects of IFNγ on particular cancer cells is important for indicating which cancers may be susceptible to IFNγ therapy (8–16).

Nasopharyngeal carcinoma (NPC) is a major malignant disease of the head and neck region and is endemic to Southeast Asia and Mediterranean basin. NPC affects a predominantly young population and the current treatment regimen of radiation therapy, even combined with cisplatin chemotherapy, yields a 5-year survival rate of ~70% (17–23). Therefore, evaluation and development of novel therapeutic approaches are critical.

To assess the potential of IFNγ in treating NPC, we carefully assessed the antitumor effects of IFNγ on NPC in a representative panel of human NPC cell lines (CNE-1, CNE-2, and C666-1; ref. 24). The results show that r-hu-IFNγ has direct antiproliferative effects on all NPC cell lines tested. However, the clinical application of recombinant IFNγ was limited by the short half-life and the systemic side effects experienced by patients. Therefore, we sought to evaluate the antitumor activity of minicircle-mediated intratumoral IFNγ gene transfer in the present study.

Minicircles are a novel form of supercoiled DNA molecule for nonviral gene transfer, which have neither bacterial origin of replication nor antibiotic resistance gene (25–30). They are generated in *E. coli* by site-specific recombination. Minicircles are superior to standard plasmid in terms of biosafety, improved gene transfer, and potential bioavailability (25, 26). The efficiency of gene transfer with minicircle vectors has been evaluated both *in vitro* in transformed primary cells and *in vivo* in liver, muscle, and experimental tumors (25–28). However, to date, minicircle vectors have never been applied in antitumor gene therapy.

Authors' Affiliations: [1]State Key Laboratory of Oncology in South China, Cancer Center, Sun Yat-sen University, Guangzhou, PR China; [2]Department of Endocrinology, Chengdu Army General Hospital, Chengdu, PR China; and [3]Institute of Microbiology, Chinese Academy of Science, Beijing, PR China

Received 3/3/06; revised 5/9/06; accepted 5/19/06.

Grant support: National Basic Research Program of China (973 Program) grant 2004CB518801, the China Postdoctoral Science Foundation grant 2004036155, and the Key Research Grant of Guangdong Province grant 2003A10902.

The costs of publication of this article were defrayed in part by the payment of page charges. This article must therefore be hereby marked *advertisement* in accordance with 18 U.S.C. Section 1734 solely to indicate this fact.

Requests for reprints: Wenlin Huang, Cancer Center, Sun Yat-sen University, Guangzhou 510060, PR China. Phone: 86-20-8734-3178; Fax: 86-20-8734-3146; E-mail: wl_huang@hotmail.com.

doi:10.1158/1078-0432.CCR-06-0520

In this study, we have developed a minicircle DNA vector carrying the IFNγ gene. The results show that IFNγ gene transfer exerts a profound antiproliferative effect on NPC cell lines by inducing G_0-G_1 phase arrest and apoptosis. Furthermore, intratumoral injections of minicircle-IFNγ significantly inhibit the growth of NPC xenografts. Compared with corresponding conventional plasmids, the minicircle vector has greater potential for antitumor gene therapy for NPC due to its capability of mediating persistent high levels of IFNγ gene expression.

Materials and Methods

Reagents. Restriction enzymes and DNA Ligation Kit were purchased from Promega (Madison, WI) and Takara (Dalian, China). DNA

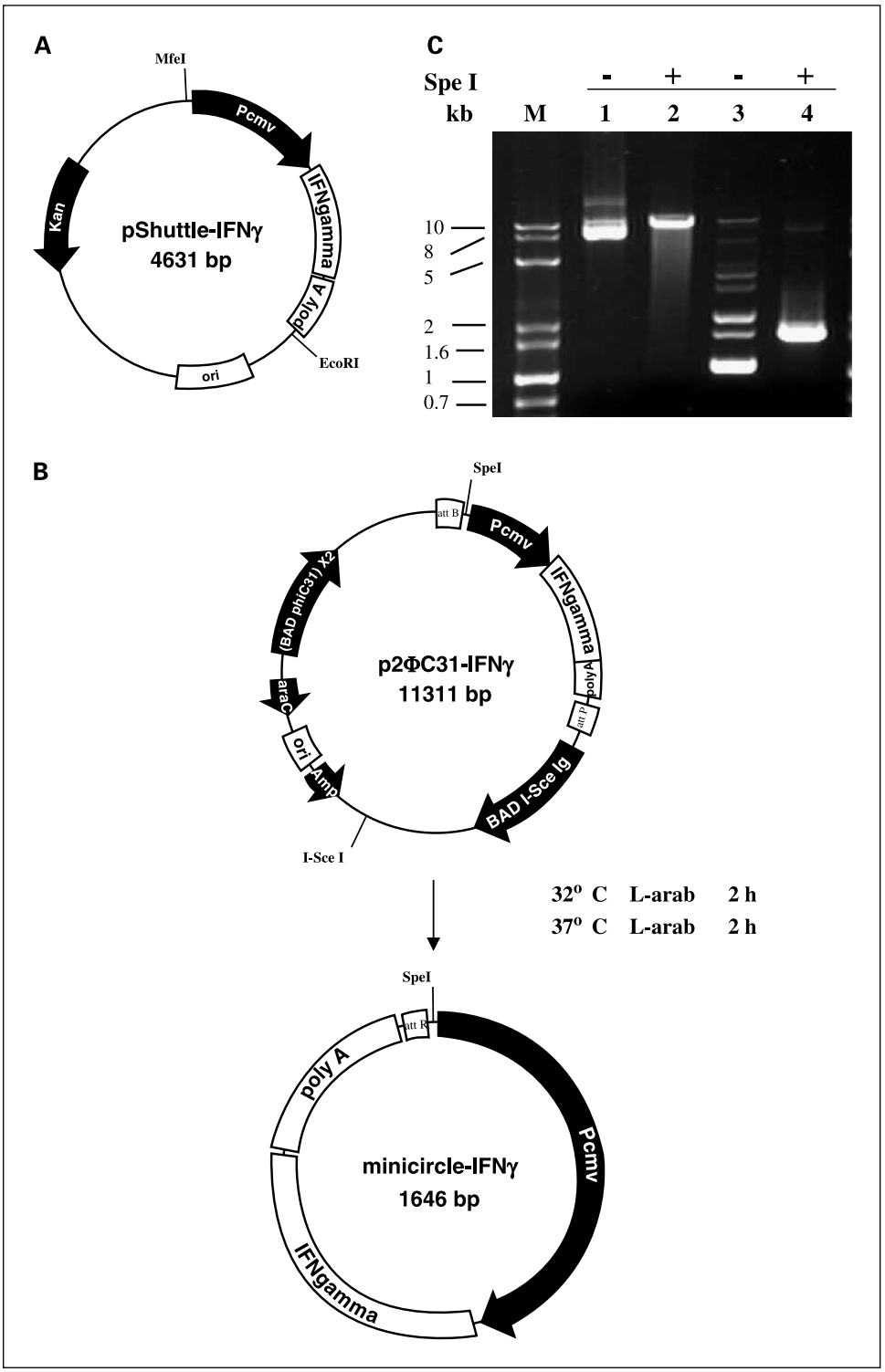

Fig. 1. Construction of p2ΦC31-IFNγ and production of minicircle-IFNγ. *A,* restriction map of pShuttle-IFNγ. P_{CMV}, immediate-early human cytomegalovirus enhancer/promoter; IFNγ, human γ interferon gene; poly A, bovine growth factor polyadenylation signal; Kan, kanamycin resistance gene; ori, pUC origin of DNA replication. *B,* flow chart of ΦC31 integrase – mediated intramolecular recombination of p2ΦC31-IFNγ. The resulting product is minicircle-IFNγ. Amp, ampicillin resistance gene; BAD, araBAD promoter; araC, araC repressor; attB, bacterial attachment site; attP, phage attachment site; attR, right hybrid sequence; I-SceIg, *I-Sce* I gene. *C,* analysis of minicircle DNA. M, 1 kb plus DNA ladder, bands of 10, 8, 5, 2, 1.6, 1, and 0.7 kb. All lanes were loaded with 0.3 μg of DNA. Lane 1, p2ΦC31-IFNγ; lane 2, p2ΦC31-IFNγ/*Spe*I; lane 3, minicircle-IFNγ; lane 4, minicircle-IFNγ/*Spe*I.

Table 1. Treatment regimens for *in vitro* and *in vivo* transfections

(A) Treatment regimen used to transfect cells with DNA constructs with the same ratio of Lipofectamine 2000 to DNA in each case (1:1)

Group	Treatment per well
p2ΦC31-IFNγ 11.3 kb	1 μg
Minicircle-IFNγ 1.6 kb	
mc-A (weight:weight)	1 μg
mc-B (mole:mole with stuffer DNA)	0.14 μg + 0.86 μg pSP72
mc-C (mole:mole without stuffer DNA)	0.14 μg
pShuttle-IFNγ 4.6 kb	1 μg

(B) Treatment regimen used for NPC-xenografted mice

Group	Treatment
0.9% NaCl	100 μL/d
Lipofectamine*	60 μL/wk
p2ΦC31 + Lipofectamine*	15 μg p2ΦC31 + 60 μL Lipofectamine/wk
r-hu-IFNγ*	100×10^4 IU/kg/d
p2ΦC31-IFNγ*	15 μg p2ΦC31-IFNγ + 60 μL Lipofectamine/wk
mc-A*	15 μg minicircle-IFNγ + 60 μL Lipofectamine/wk
mc-B*	2.1 μg minicircle-IFNγ + 12.9 μg pSP72 + 60 μL Lipofectamine/wk

*0.9% NaCl solution was added to adjust the total volume to 100 μL.

ladder (1 kb Plus) was purchased from TianWei Technology Co. Ltd. (Shanghai, China). Lipofectamine 2000 was obtained from Invitrogen (Carlsbad, CA). L-Arabinose was purchased from Sigma (St. Louis, MO). r-hu-IFNγ (200×10^4 IU/vial) was obtained from Shanghai Clone Technology Co. Ltd. (Shanghai, China). It was diluted in water and stored in aliquots at −70°C. The specific activity was 2×10^7 units/mg protein.

Plasmids and strains. Plasmid p2ΦC31 (9.7 kb) was a kind gift from Dr. Zhiying Chen (Stanford University, Stanford, CA). Plasmid pShuttle-IFNγ (4.6 kb) carrying the human IFNγ expression cassette was constructed by our lab. pSP72 was obtained from Promega. The *E. coli* strains *DH 5α* and *Top 10* were purchased from Invitrogen.

Production and purification of minicircle-IFNγ. Minicircle-IFNγ was produced according to methods described by Chen et al. (30) with minor modifications. Overnight bacterial growth from a single colony of plasmid-transformed *E. coli Top 10* in Tris-borate medium was centrifuged at 20°C, 4,000 rpm for 20 minutes. The pellet was resuspended 4:1 (v/v) in fresh Luria-Bertani broth containing 1.5% L-arabinose. The bacteria were incubated at 32°C with constant shaking at 250 rpm for 2 hours. After adding one-half volume of fresh Luria-Bertani broth (pH 8.0) containing 1% L-arabinose, the incubation temperature was increased to 37°C and the incubation continued for an additional 2 hours. Episomal DNA circles were prepared from bacteria using plasmid purification kits from Qiagen (Chatsworth, CA).

In vitro *gene transfer.* Five cell lines were studied: 293 (human embryonic kidney cell line), NIH 3T3 (murine fibroblast cell line), CNE-1 (well-differentiated NPC cell line, EBV negative), CNE-2 (poorly-differentiated NPC cell line, EBV negative), and C666-1 (undifferentiated NPC cell line, EBV positive). The doubling time of CNE-1 and CNE-2 was ~20 to 24 hours and that of C666-1 was ~3.5 days (21–24). Experiments were carried out in the log phase of growth. Cells were cultured in RPMI 1640 containing 100 units/mL penicillin, 100 μg/mL streptomycin, and 10% fetal bovine serum (Gibco, Paisley, United Kingdom) at 37°C in a 5% CO_2 humidified atmosphere. C666-1 is a kind gift from Dr. Saiwah Tsao (University of Hong Kong, Hong Kong, PR China). 293, NIH 3T3, CNE-1, CNE-2, and WISH cell lines were kept by this lab.

For transfection, confluent cells were treated with trypsin and seeded into 24-well microtiter plates in 1 mL of 10% fetal bovine serum-RPMI 1640. Cells were transfected 18 hours after seeding for 293, NIH 3T3, CNE-1, and CNE-2, and 72 hours for C666-1 at 50% to 60% confluence. Transfection was conducted according to the instruction of the manufacturer (Lipofectamine 2000, Invitrogen). Cells were then incubated for varying lengths of time.

IFNγ production by minicircle-IFNγ transfected cell lines. The concentration of IFNγ in the culture supernatant of transfected cell lines was measured with a human IFNγ ELISA kit (R&D Systems, Minneapolis, MN) according to the recommendations of the manufacturer.

Activity assay of IFNγ produced by minicircle-IFNγ transfected cell lines. The culture supernatant of NPC cells treated with minicircle-IFNγ for 72 hours was collected and frozen (−70°C) for activity analysis. Activity of IFNγ was measured according to the method described by Ahmed et al. (31) with minor modifications. The viability of WISH cells was determined by 3-(4,5-dimethylthiazol-2-yl)-2,5-diphenyltetrazolium bromide assay. r-hu-IFNγ (20 IU/ng) produced by *E. coli* was used as standard.

WST assay. The nature of C666-1 cells precluded the use of clonogenic survival assay; therefore, WST assay was used to assess the effect of IFNγ gene transfer on the growth of the NPC cell lines (21–24, 32). We transfected three different NPC cell lines with minicircle-IFNγ and corresponding control plasmids. After the indicated incubation periods, cell viability was measured with Cell Counting Kit-8 (Dojindo Molecular Technologies, Inc., Gaithersburg, MD) according to the instruction of the manufacturer.

Flow cytometry. After treatment for the indicated time courses, adherent and detached cells were harvested and fixed overnight with 70% ethanol at 4°C, followed by resuspension in 500 μL of PBS. After addition of 10 μL RNase (10 mg/mL), cells were left for 30 minutes at 37°C and stained with 10 μL propidium iodide (1 mg/mL). Cellular DNA content was determined for at least 1×10^5 cells on a Coulter Epics Elite flow cytometer (Beckman-Coulter, Miami, FL). Cell cycle

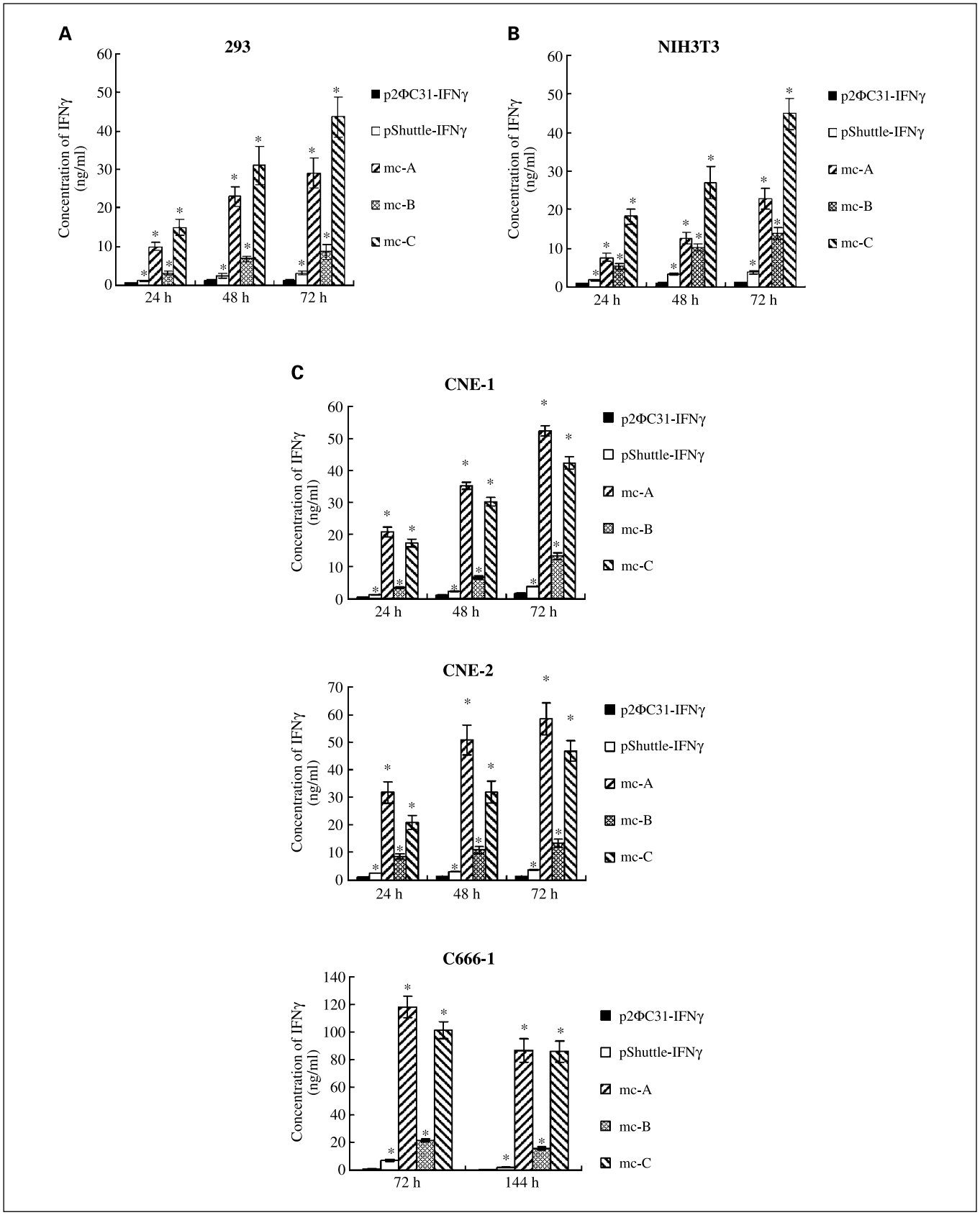

Fig. 2. Expression profiles of IFNγ in the supernatant of cells transfected with plasmids carrying human IFNγ expression cassette. Transfections were done with the same amount of total DNA and same molarities of IFNγ-cassette with or without stuffer DNA. *A* to *C,* columns, mean of three independent experiments, each conducted in triplicate; bars, SE. *, $P < 0.05$, compared with p2ΦC31-IFNγ – treated group.

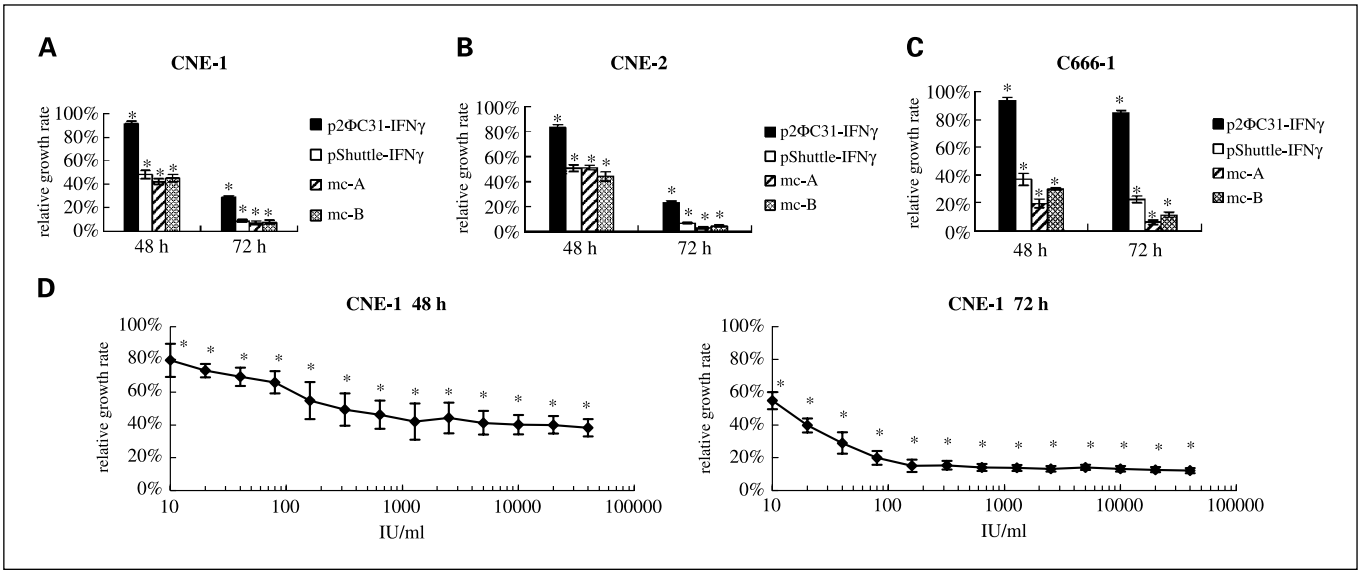

Fig. 3. IFNγ gene transfer inhibits *in vitro* growth of human NPC cells. Cells were treated with minicircle-IFNγ and control plasmids for the indicated time periods. Cell viability was determined by WST assay. Data are given as relative growth rates compared with p2ΦC31-treated group. *A* to *C,* columns, mean of three independent experiments, each conducted in triplicate; bars, SE. *, $P < 0.05$, compared with p2ΦC31-treated group. *D,* r-hu-IFNγ inhibits *in vitro* growth of CNE-1 cell line. Cells were treated with r-hu-IFNγ at doses ranging from 10 to 40,000 IU/mL for indicated time periods. Points, mean of three independent experiments, each conducted in triplicate; bars, SE. *, $P < 0.05$, compared with cells treated with medium alone.

analysis was done with the Multicycle system (Phoenix Flow Systems, San Diego, CA).

Caspase-3 activity assay. Cells were plated in 15-cm dishes. Floating and adherent cells were harvested and combined for apoptosis assays. Caspase-3 activity was determined with Caspase-3 Cellular Activity Assay Kit (Calbiochem, La Jolla, CA).

Effect of minicircle-IFNγ treatment on the growth of NPC xenografts. Female BALB/c nude mice (4-6 weeks old) were obtained from Shanghai Slike Experimental Animals Co. Ltd. (Shanghai, China; animal experimental license no. SCXKhu2003-0008). After 1 week of adaptation, mice were inoculated s.c. in the scapular region with 2×10^6 CNE-2 cells or 1×10^7 C666-1 cells to generate tumors for the following experiments. When 30- to 40-mm^3 tumors had formed, mice were randomly assigned to groups. For antitumor experiments, a total of 35 mice were used for either xenograft model (5 mice per group, 7 groups). Tumor tissues received injections of plasmids packaged with Lipofectamine for the experimental groups. Tumor volume (V) was measured and calculated according to the following formula: $V = L \times W^2/2$ (L, length; W, width). Tumors were resected at the end point and frozen (−70°C) for analysis. For intratumoral expression analysis, mice were treated with minicircle-IFNγ or p2ΦC31-IFNγ. There were 60 mice in total, which were divided into four groups. Three mice for each time point (days 1, 3, 7, 14, and 21) were tested. Tumors were resected at indicated day and frozen (−70°C) for analysis. For survival studies, there were 10 mice in each group. Seven treatment groups were included for either xenograft model. Animals either were found dead or were sacrificed when tumors were observed by palpation to approach 10% body weight or individual animals seemed to be stressed by weight loss, ruffled fur, and/or lethargy. All the animal experiments were conducted in accordance with Guidelines for the Welfare of Animals in Experimental Neoplasia.

RNA preparation and reverse transcription-PCR. Total RNA was prepared using Micro-to-Midi Total RNA Purification System (Invitrogen) according to the instruction of the manufacturer. RNA was submitted to DNase digestion and aliquots of 1 μg were used for reverse transcription with Reverse Transcription System (Promega). PCR reactions were done using the following primers: mouse β-actin, sense 5′-GTGGGCCGCTCTAGGCACCA-3′ and antisense 5′-CGGTTGGCCTTAGGGTTCAGGGGGG-3′; human IFNγ, sense 5′-CCCTCTAGATGTTACTGCCAGGACCCATA-3′ and antisense 5′-CCCGCGGCCGCTTACTGGGATGCTCTTCGAC-3′. Cycle conditions for all PCR reactions were 1 minute at 95°C, 1 minute at 55°C, and 1 minute at 72°C for 30 cycles. The size of expected PCR products was 250 bp for β-actin and 460 bp for IFNγ. As confirmed by our lab, a 350-bp product for β-actin will emerge if there was any DNA contamination.

IFNγ production by minicircle-IFNγ transfected tumor tissues. Frozen samples were ground in 1× TBS (25 mmol/L Tris, 138 mmol/L NaCl, and 3 mmol/L KCl, pH 7.4) and centrifuged at 8,000 × g for 1 minute. The supernatants were used for analysis. IFNγ levels were determined with a human IFNγ ELISA kit (R&D Systems) according to the recommendation of the manufacturer.

Statistical analysis. Results were evaluated using t test with SPSS 11.0 software (SSPS, Inc., Chicago, IL), unless otherwise specified. Results of survival were evaluated using Kaplan-Meier. $P < 0.05$ was considered statistically significant.

Results

Construction of p2ΦC31-IFNγ. Plasmid pShuttle-IFNγ carried the human IFNγ gene expression cassette (Fig. 1A). This construct (4.6 kb) has the following components: the pUC origin of replication, a kanamycin resistance gene, the IFNγ gene under the control of immediate-early human cytomegalovirus promoter, and a bovine growth hormone gene polyadenylation signal (Fig. 1A).

To prepare the human IFNγ minicircle-producing construct p2ΦC31-IFNγ (Fig. 1B), we inserted the 1.6-kb *Mfe*I-P_{CMV}/IFNγ/poly(A)-*Eco*RI fragment from pShuttle-IFNγ into the *Eco*RI site of pCI, resulting in an intermediate plasmid, pCI-IFNγ (data not shown). The parent plasmid p2ΦC31-IFNγ (11.3 kb) was created by insertion of the 1.6-kb *Sal*I-P_{CMV}/IFNγ/poly(A)-*Xho*I fragment of pCI-IFNγ into the *Xho*I site of p2ΦC31 (9.7 kb). All constructs were confirmed by DNA sequencing.

Production and purification of minicircle-IFNγ. Minicircle-IFNγ (1.6 kb) was produced and purified (Fig. 1B). Parent plasmid p2ΦC31-IFNγ and the recombinant product minicircle-IFNγ were shown in lanes 1 and 3, respectively (Fig. 1C). The purity of minicircle-IFNγ was analyzed by agarose gel electrophoresis (Fig. 1C). Weak p2ΦC31-IFNγ band and bacterial backbone contamination were barely detectable in lanes 3 and 4. Integrated density analysis revealed that the purity was 96%. We also examined the quality of the resulting minicircle-IFNγ by comparing the agarose gel migration patterns of cut and uncut minicircle-IFNγ (Fig. 1C). The results indicate that most of the minicircle-IFNγ were supercoiled with small amounts of nicked form, linear form, and dimer.

IFNγ production by transfected cell lines. Comparative tests were done to investigate the efficiency of the minicircle DNA vector. We compared minicircle-IFNγ with its parent plasmid p2ΦC31-IFNγ, as well as with the origin plasmid from which p2ΦC31-IFNγ was derived (pShuttle-IFNγ), all of which contained an IFNγ expression cassette driven by a cytomegalovirus promoter (Fig. 1).

293 cells, NIH 3T3 cells, and three NPC cell lines were transfected according to the regimen shown in Table 1A (27). The culture supernatant of each treatment was collected to investigate the cumulative production of IFNγ over the indicated time course. The expression profile of IFNγ in 293 cells was shown in Fig. 2A. No IFNγ was found in the culture medium from p2ΦC31- or pSP72-transfected 293 cells (data not shown).

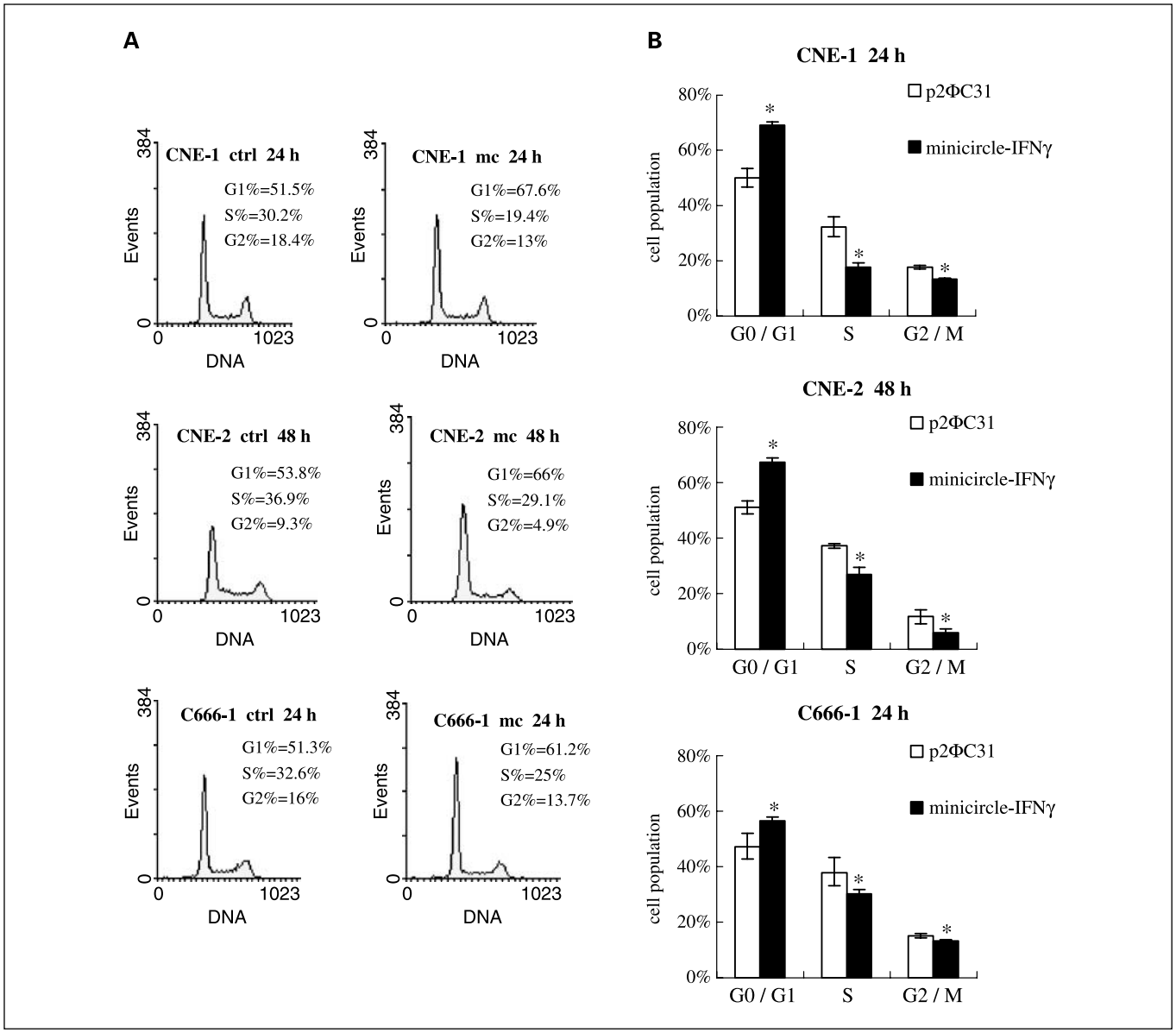

Fig. 4. IFNγ gene transfer exerts antiproliferative effects on NPC cells by inducing G_0-G_1 arrest and apoptosis. *A* and *B,* cell cycle phase distribution of minicircle-IFNγ – treated NPC cell lines. Three NPC cell lines were transfected with minicircle-IFNγ and the cell cycle phase distribution of each cell lines was analyzed at the indicated time. *A,* data from representative flow cytometry experiments at indicated time point after transfection. Ctrl, p2ΦC31-treated group; mc, minicircle-IFNγ treated group. *B,* graphical representation of the mean total population in each stage of the cell cycle. Columns, mean of three independent experiments; bars, SD. *, $P < 0.05$, compared with p2ΦC31-treated group.

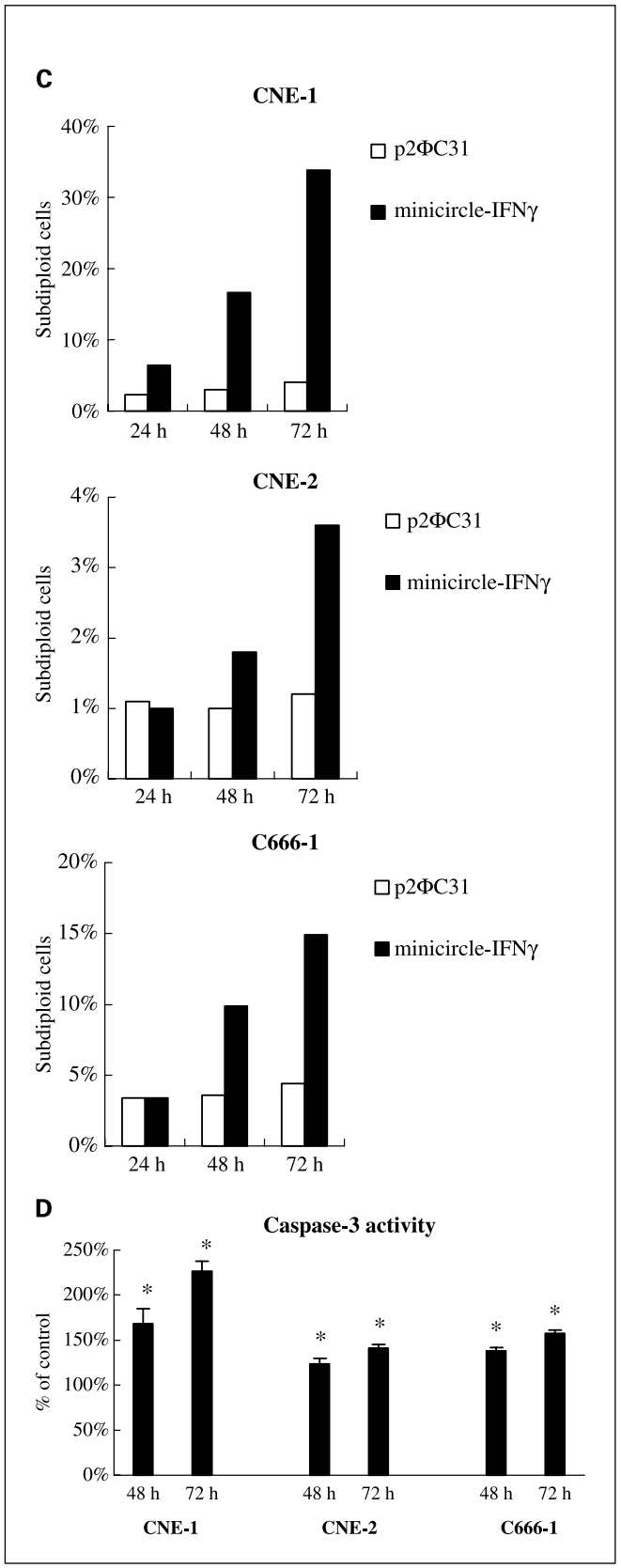

Fig. 4 *Continued. C,* graphical representation of the percentage population in pre-G_1 phase from a representative experiment. *D*, caspase-3 activity induced by IFNγ gene transfer. Columns, mean of three independent experiments; bars, SD. *, $P < 0.05$, compared with p2ΦC31-treated group.

As shown in Table 1A, cells treated with minicircle-IFNγ were divided into three groups: mc-A group (treatment of weight:weight), mc-B group (treatment of mole:mole with stuffer DNA), and mc-C group (mole:mole without stuffer DNA treatment). Compared with p2ΦC31-IFNγ group, equal weights of DNA and equal amounts of Lipofectamine were used in mc-A group. For mc-B group, equal numbers of IFNγ expression cassettes and same amount of Lipofectamine were used. For mc-C group, equal numbers of IFNγ expression cassettes and same ratio of DNA to Lipofectamine were used.

The treatment of weight:weight (mc-A) compared equal weights of DNA from minicircle and parent plasmid (27). The amount of Lipofectamine was the same but the amount of IFNγ expression cassette of minicircle was 6.1 times higher than in p2ΦC31-IFNγ and 1.9 times higher than in pShuttle-IFNγ. Seventy-two hours after transfection, the yield of IFNγ mediated by the minicircle was 20.6 times higher than in p2ΦC31-IFNγ and 8.3 times higher than in pShuttle-IFNγ (Fig. 2A).

The treatment of mole:mole with stuffer DNA (mc-B) compared equal molar ratios of DNA from each construct (27). pSP72 was used as stuffer DNA to adjust the DNA amount of each well to 1 μg. Equal amounts of Lipofectamine were used to minimize variation in Lipofectamine-induced cytoxicity. In this treatment, the expression level in minicircle, 72 hours after transfection, was 5.4 times higher than in p2ΦC31-IFNγ and 1.7 times higher than in pShuttle-IFNγ (Fig. 2A).

The mole:mole without stuffer DNA treatment (mc-C) allowed comparison of molar ratios of constructs with variable Lipofectamine quantities (27). The expression level of the mc-C group was significantly higher than that of the mc-A or mc-B group (Fig. 2A; $P < 0.05$). This effect is likely due to lower levels of Lipofectamine-induced cytoxicity in the mc-C group.

In all, IFNγ expression in 293 cells mediated by minicircle was significantly higher than those in control plasmids ($P < 0.05$). Similar results were obtained in NIH 3T3 cells (Fig. 2B). In addition, with the exception of mc-C group, similar results were also obtained in all three NPC cell lines (Fig. 2C).

In contrast to 293 and NIH 3T3 cells, the expression levels of IFNγ in the mc-C group of the three NPC cells were between those of mc-A group and mc-B group (Fig. 2C). The data indicate that NPC cells were less sensitive to Lipofectamine-induced cytoxicity than 293 and NIH 3T3 cells.

Antiproliferative effects of IFNγ gene transfer on human NPC cell lines. We previously investigated the antiproliferative activity of r-hu-IFNγ in three EBV-positive or EBV-negative NPC cell lines (CNE-1, CNE-2, and C666-1). The results suggested that IFNγ treatment significantly inhibited the growth of all NPC cell lines. The IC_{50} values of CNE-1, CNE-2, and C666-1 were 12.9, 43.9, and 167.3 IU/mL, respectively, after being treated with r-hu-IFNγ for 72 hours. Concerned about the limitation of the recombinant protein in clinical application, in the present study, we sought to assess the potential of IFNγ gene therapy on NPC.

To evaluate the efficiency of gene transfer and the capability of the NPC cells to produce the transgene, we investigated cumulative IFNγ production over the indicated time course (Fig. 2C). The activity of IFNγ produced by transfected CNE-1, CNE-2, and C666-1 was also determined, which was 27.9, 46.7, and 33.1 IU/ng, respectively. Therefore, all NPC cell lines transfected with minicircle-IFNγ produced amounts of IFNγ greater than their IC_{50}.

Furthermore, to examine whether IFNγ gene transfer has the same effect on the growth of the NPC cell lines, CNE-1, CNE-2, and C666-1 were transfected with minicircle-IFNγ and control plasmids according to the regimen shown in Table 1A. WST assays were conducted after one to three doubling time. No significant differences between the growth of p2ΦC31 + Lipofectamine– or Lipofectamine-treated group and untreated group were observed (data not shown). Consistent with our observations from r-hu-IFNγ treatment, growth inhibition was notably absent during the first day after transfection (data not shown) but became apparent on day 2 for CNE-1 and CNE-2 and on day 3 for the slower-growing C666-1 (Fig. 3). Although both of the plasmids carried the same IFNγ cassette and inhibited the growth of cells significantly ($P < 0.04$), minicircle showed more profound effects than the parent plasmid ($P < 0.006$). For example, 48 hours after transfection, the cell viability of CNE-2 in mc-A group was reduced to 51.0 ± 1.8%, compared with 83.0 ± 2.6% of p2ΦC31-IFNγ group (Fig. 3B). Additionally, the relative growth rates of these two groups were further decreased to 2.7 ± 1.0% versus 22.9 ± 1.4%, respectively, 72 hours after transfection (Fig. 3B).

Although the IFNγ expressions of pShuttle-IFNγ, mc-A, and mc-B groups were significantly different (Fig. 2C; $P < 0.008$), all groups exerted similar effects on the growth of CNE-1 and CNE-2 cells by 72 hours (Fig. 3A and B; $P > 0.05$). This was likely due to the dose-dependent inhibitory effects of IFNγ treatment on NPC cell lines. As shown in Fig. 3D, r-hu-IFNγ treatment inhibited the growth of CNE-1 in a dose-dependent manner, which showed a sigmoidal dose-response curve, and the maximal inhibition was achieved at doses below the highest dose tested. A similar result was obtained in CNE-2 cell line (data not shown). Therefore, the yield of IFNγ in pShuttle-IFNγ and mc-B groups was high enough to achieve antiproliferative effects similar to that in mc-A group.

In contrast to NPC cell lines, no growth inhibitory effect was observed in 293 and NIH 3T3 cells treated with IFNγ gene transfer (data not shown). We also tested a human hepatocarcinoma cell line (HepG2) and a human colon carcinoma cell line (Lovo) in this work. No significant antiproliferative effect was observed in these two cell lines, although they achieved similar expression levels of IFNγ with NPC cell lines (data not shown).

IFNγ gene transfer induces cell cycle arrest in NPC cell lines. NPC cell lines were transfected with minicircle-IFNγ as the method described above and cells were collected at indicated time points. The cell cycle phase distribution was evaluated by flow cytometric analysis. The results revealed that IFNγ gene transfer arrested NPC cells in the G_0-G_1 phase of the cell cycle (Fig. 4A and B). A significant increase of cells in G_0-G_1 phase could be detected in CNE-1 and C666-1 by 24 hours and in CNE-2 by 48 hours ($P < 0.02$). For example, 67.6% of CNE-1 cells accumulated in the G_0-G_1 phase 24 hours after transfection, in contrast to 51.5% for p2ΦC31-transfected cells (Fig. 4A). This was associated with corresponding decreases in proportion of cells in S phase (from 30.2% to 19.4%) and G_2-M phase (from 18.4% to 13%; Fig. 4A). Similar alterations, but to a lesser extent, were observed in the other two NPC cell lines (Fig. 4A and B). The effects of IFNγ gene transfer on cell cycle phase distribution were consistent with that observed with r-hu-IFNγ treatment (data not shown).

IFNγ gene transfer induces apoptosis in NPC cell lines. Flow cytometry analysis revealed an increased percentage of cells with subdiploid DNA content at 48 and 72 hours (Fig. 4C), suggesting an induction of apoptosis. For example, 72 hours after treatment, the percentage of CNE-1 cells in pre-G_1 peak was 33.8%, as compared with 4% of the control group. Similar results were obtained from CNE-2 and C666-1 (Fig. 4C).

As the pre-G_1 peak did not provide conclusive evidence of apoptosis, we investigated IFNγ-induced activation of caspase-3 to evaluate whether an induction of apoptosis contributed to the antiproliferative effects of IFNγ. The caspase-3 activity assay revealed a significant increase of activity by 48 hours for the three cell lines ($P < 0.03$). Moreover, there was further induction of the caspase-3 activity by 72 hours, which strongly suggests an involvement of apoptosis in the antiproliferative effects of IFNγ gene transfer (Fig. 4D).

IFNγ gene transfer inhibits the growth of human NPC xenografts. Because the majority of NPC biopsies belong to undifferentiated cell type, C666-1 and CNE-2 were focused on for *in vivo* antitumor study (21–24).

CNE-2 cell– and C666-1 cell–xenografted mice were treated for 3 weeks, according to the regimen shown in Table 1B. The first three groups shown in Table 1B were treated as negative controls and the r-hu-IFNγ group was treated as a positive control. For the IFNγ gene treatment, *in vivo* transfections were done with the same amount of total DNA and the same molarities of IFNγ-cassette with stuffer DNA (Table 1B).

The experiments were conducted twice. Results of representative experiments were presented. The time-dependent evolution of tumor volume in mice inoculated with CNE-2 and C666-1 cells is shown in Fig. 5A. The results indicated that the sizes of tumors treated with IFNγ gene therapy or r-hu-IFNγ were significantly decreased compared with control groups ($P < 0.05$). No significant differences in the size of three negative control groups were observed ($P > 0.05$).

The inhibition rate of the treated group was determined according to tumor weight (Fig. 5B) and the growth of tumors after IFNγ gene therapy or r-hu-IFNγ treatment was significantly slower those of the control groups ($P < 0.05$). In the CNE-2 cell–xenografted models, the inhibition rates of mc-A, mc-B, p2ΦC31-IFNγ, and r-hu-IFNγ groups were 77.5%, 50.7%, 32.4%, and 43.7%, respectively. For the C666-1 cell–xenografted models, the corresponding inhibition rates were 83%, 75.5%, 58.5%, and 64.2%, respectively. In both models, the mc-A group showed more profound antitumor potential than the parent plasmid–treated group ($P < 0.004$; Fig. 5B). No significant differences in the weight of three negative control groups were observed ($P > 0.05$).

Although p2ΦC31-IFNγ exerted slight antiproliferative effects on C666-1, an inhibition rate of 58.5% was achieved by intratumoral injection. This effect is likely due to the indirect antitumor, antiangiogenesis effect of IFNγ because we have found that the microvessel densities of the treated tumors were significantly decreased compared with negative control groups (data not shown).

IFNγ production by transfected tumor tissues. To compare the persistence of gene expression, expression of IFNγ transcript and protein was evaluated on days 1, 3, 7, 14, and 21 after single administration, respectively (Fig. 5C). Transfection was conducted with the same protocol as with the mc-A and

p2ΦC31-IFNγ groups shown in Table 1B, except for the injection frequency. The treated mice just received one injection during 3 weeks.

The data suggest that minicircle-IFNγ is capable of expressing persistent high ($P < 0.05$) levels of IFNγ *in vivo* (Fig. 5C). For example, the expression level of mc-A group was 11 to 14 times higher than that of p2ΦC31-IFNγ–treated group in CNE-2- and C666-1-xenografted models 1 day after DNA injection (Fig. 5C). The expression of IFNγ transcript and protein could be detected on day 21 in the mc-A group whereas they were

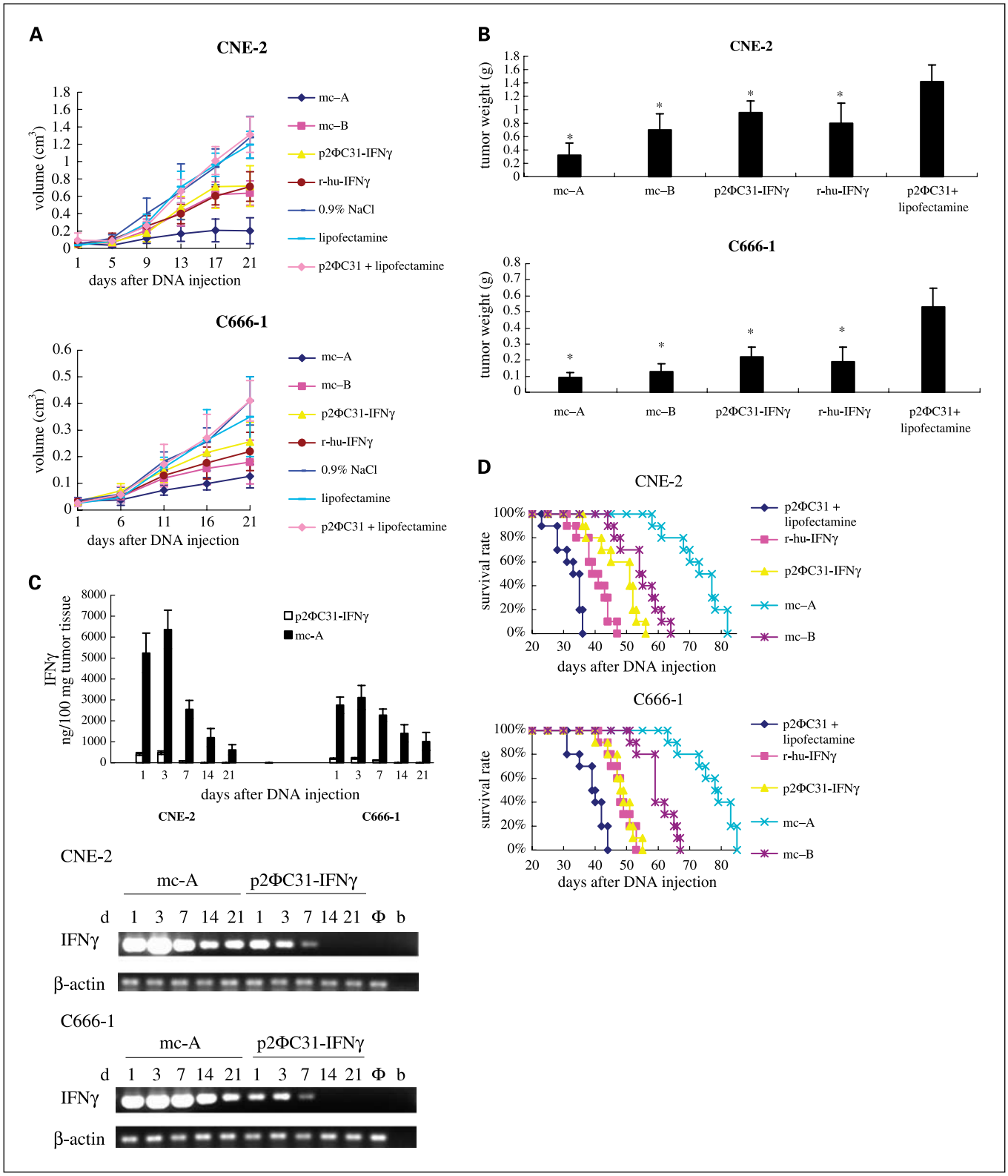

barely detectable on day 7 and undetectable on day 14 in the p2ΦC31-IFNγ group (Fig. 5C). No IFNγ transcript or protein was found in p2ΦC31-treated group or untreated tumors.

Mice received three doses (one dose per week for 3 weeks) were also tested in intratumoral expression experiments. Transfection was conducted with the same protocol as with the mc-A group shown in Table 1B. For CNE-2 cell–xenografted mice, the expression levels of IFNγ in single-dose group and three-dose group were 1,197.7 ± 441 and 3,105.5 ± 535.3 ng/100 mg tumor tissue on day 14 ($P > 0.05$, one dose versus three doses). The corresponding expression levels were 617.3 ± 240.7 and 3,559.4 ± 686.8 ng/100 mg tumor tissue on day 21 ($P < 0.04$, one dose versus three doses). Tumor volumes were recorded to assess the antitumor effects of these two treatment groups. Results indicated that the sizes of tumors in both groups were significantly decreased on day 21 ($P < 0.05$). Compared with one-dose treatment, three-dose treatment achieved significantly high production of IFNγ ($P < 0.04$) and better antitumor effect on day 21 (0.873 ± 0.119 versus 0.315 ± 0.068 cm^3; $P < 0.01$, one dose versus three doses).

Similar results of intratumoral expression were obtained in C666-1 cell–xenografted mice. Mice in three-dose group achieved significantly high production of IFNγ on day 21 (1,016.8 ± 427.9 versus 3,451.5 ± 600.8 ng; $P < 0.01$, one dose versus three doses). The sizes of tumors in both groups were significantly decreased on day 21 ($P < 0.05$). However, although the mean tumor volume in three-dose group was smaller than that in single-dose group, the difference was not significant (0.229 ± 0.046 versus 0.162 ± 0.045 cm^3; $P > 0.05$, one dose versus three doses).

IFNγ gene transfer increases the survival of human NPC–xenografted mice. The long-term outcome of IFNγ gene transfer was evaluated by survival rates of mice with the same protocol shown in Table 1B. There was no additional treatment after 3 weeks of treatment. The experiments were conducted twice. Results of representative experiments were shown in Fig. 5D. For CNE-2 cell–xenografted mice, the median survival of p2ΦC31 + Lipofectamine, r-hu-IFNγ, p2ΦC31-IFNγ, mc-A, and mc-B groups was 32 ± 1.58, 38 ± 2.37, 50 ± 4.65, 76 ± 2.83, and 53 ± 3.69 days, respectively (Fig. 5D). For C666-1 cell–xenografted mice, the corresponding median survival was 38 ± 3.56, 47 ± 0.77, 47 ± 1.58, 77 ± 3.16, and 58 ± 2.32 days, respectively (Fig. 5D). In both models, no significant differences in the survival of three negative control groups were observed ($P > 0.05$, Kaplan-Meier; Fig. 5D). Survival durations were significantly longer after IFNγ gene therapy or r-hu-IFNγ treatment than in negative control groups ($P < 0.0007$, Kaplan-Meier; Fig. 5D). Furthermore, the mc-A group had the best survival duration ($P < 0.0002$, Kaplan-Meier; Fig. 5D).

Discussion

IFNγ has been investigated as a potential therapy for many types of cancerous tumors, such as hairy cell leukemia, chronic myelogenous leukemia, malignant melanoma, and ovarian cancer (1–5, 33–38). In the current study, we report for the first time that minicircle-mediated IFNγ gene transfer has direct antiproliferative effects on human NPC cell lines and xenografts in nude mice.

Three NPC cell lines (CNE-1, CNE-2, and C666-1) were investigated in our study. As the latent form of EBV is constantly present in >80% of NPC patients, C666-1 is unique in the tested cell lines in that it has been shown to maintain EBV in long-term cultures (24). Despite the latent EBV product present in C666-1, the antiproliferative effect of IFNγ gene therapy was as profound as that observed in EBV-negative cell lines. It is notable that C666-1 is a good tool for investigating interactions between EBV latent products and the IFNγ-induced signal pathway.

The antiproliferative mechanisms by which IFNγ exerts its effects seem to be cell type specific (6, 7, 10–16, 39–42). In pancreatic cancer cells, IFNγ induces apoptosis (8), and in prostate cancer cells, it induces cell cycle arrest (9). Here we report that both G_0-G_1 phase arrest and apoptosis contributed to IFNγ-mediated growth suppression in NPC cell lines. The G_0-G_1 phase arrest induced by IFNγ gene transfer may be due to differential regulation of cell cycle–associated proteins that control the G_1-S checkpoint (6). Moreover, IFNγ can induce apoptosis through up-regulation of the expression of a number of apoptosis-related proteins, including tumor necrosis factor receptor, Fas, and other death receptors, as well as their respective ligands, several Bcl-2 family members, and caspases in different cell types (43–48). Elucidation of the underlying mechanisms will help to develop combinatorial strategies involving IFNγ and other therapeutic agents (43–48).

As IFNγ is a multifunctional cytokine, the mechanism by which it achieves antitumor effects is complicated. In the intact host, the actions of IFNγ involve a combination of direct actions on tumor cells, inhibition of angiogenesis, and regulation of immunologic responses (1–5). It remains to be evaluated whether the two indirect actions are involved in the antitumor effect of IFNγ gene therapy in NPC. Our observations from the antitumor experiments showed that microvessel densities in tumors treated with IFNγ gene therapy were significantly decreased, which indicates that antiangiogenesis

Fig. 5. Antitumor effect of IFNγ gene transfer on growth of NPC xenografts. *A,* time-dependent evolution of tumor volume in mice inoculated with the CNE-2 and C666-1 cell lines ($n = 5$). For CNE-2 cell – xenografted mice, mc-A versus p2ΦC31 + Lipofectamine, $P < 0.05$ at days 5, 9, 13, 17, and 21; mc-B versus p2ΦC31 + Lipofectamine, $P < 0.05$ at days 17 and 21; p2ΦC31-IFNγ versus p2ΦC31 + Lipofectamine, $P < 0.05$ at days 17 and 21; r-hu-IFNγ versus 0.9% NaCl, $P < 0.05$ at days 13, 17, and 21. For C666-1 cell – xenografted mice, mc-A versus p2ΦC31 + Lipofectamine, $P < 0.05$ at days 11, 16, and 21; mc-B versus p2ΦC31 + Lipofectamine, $P < 0.05$ at days 16 and 21; p2ΦC31-IFNγ versus p2ΦC31 + Lipofectamine, $P < 0.05$ at day 21; r-hu-IFNγ versus 0.9% NaCl, $P < 0.05$ at days 16 and 21. *B,* antitumor effect of IFNγ gene therapy on CNE-2 cell – xenografted and C666-1 cell – xenografted nude mice ($n = 5$). Mice were sacrificed after 3 weeks of treatment and tumors were resected and weighted. Columns, mean of five mice; bars SD. *, $P < 0.05$, compared with p2ΦC31 + Lipofectamine – treated group. *C,* expression profiles of IFNγ and reverse transcription-PCR analysis of IFNγ transcripts in the tumor tissue transfected with minicircle-IFNγ and p2ΦC31-IFNγ. For expression profiles of IFNγ, results are given in nanograms per 100 mg of tumor tissue. Columns, mean of three mice; bars, SD. For reverse transcription-PCR analysis of IFNγ transcripts, results from representative experiments were shown. β-Actin was used as loading control. Φ, p2ΦC31 group, 1 day after injection; b, blank control. *D,* effect of IFNγ gene transfer on survival ($n = 10$). For CNE-2 cell – xenografted mice, mc-A versus p2ΦC31-IFNγ, $P < 0.0001$; mc-B versus p2ΦC31-IFNγ, $P < 0.02$; mc-A versus r-hu-IFNγ, $P < 0.0001$; mc-B versus r-hu-IFNγ, $P < 0.0001$; p2ΦC31-IFNγ versus r-hu-IFNγ, $P < 0.007$. For C666-1 cell – xenografted mice, mc-A versus p2ΦC31-IFNγ, $P < 0.0001$; mc-B versus p2ΦC31-IFNγ, $P < 0.0001$; mc-A versus r-hu-IFNγ, $P < 0.0001$; mc-B versus r-hu-IFNγ, $P < 0.0002$; p2ΦC31-IFNγ versus r-hu-IFNγ, $P > 0.05$ (Kaplan-Meier).

also contributes to IFNγ antitumor activity. Studies reveal that an IFNγ inducible protein, IP-10, functions as an inhibitor of angiogenesis and contributes to the antitumor effect of IFNγ *in vivo*. IP-10 could be induced by IFNγ in endothelial cells and exert potent antiangiogenesis activity by inhibiting endothelial cell differentiation (49, 50). However, being highly species specific, human IFNγ should not have any direct effect on the murine vascular system. Therefore, the antiangiogenesis activity of IFNγ expression may be explained by the down-regulation of angiogenic factors and/or up-regulation of antiangiogenic factors of NPC cells. Because human IFNγ has no measurable activity in the nude mouse host (37), it seems that the immunomodulation of IFNγ does not contribute to its antitumor effect. However, we cannot exclude the possibility that IFNγ expression or administration of plasmid/liposome induces a nonspecific activation of the residual immune system of nude mice.

In addition to investigating the antitumor effects of IFNγ gene transfer in NPC models, we also assessed the potential of the minicircle vector in antitumor gene therapy. The IFNγ expression profiles mediated by minicircle and classic plasmids were compared both *in vitro* and *in vivo*. Consistent with Darquet et al.'s reports (25, 26), our data show that the minicircle is more efficient in mediating *in vitro* transgene expression than the commonly used plasmid pShuttle and much more efficient than the large plasmid p2ΦC31. The minicircle-IFNγ consistently produced the highest expression when the same amount and molarity of DNA were used. The expression differences were partly cell dependent, with the largest difference being in the C666-1 cells.

Data about minicircle-mediated intratumoral gene expression are limited. There has only been one report that investigated this issue, and they found that intratumoral injection of the minicircle resulted in 13 to 50 times more gene expression than the parent plasmid or large plasmids when the same amount of DNA was used (26). Accordingly, we found that minicircle-IFNγ achieved 11 to 14 times higher IFNγ expression than p2ΦC31-IFNγ in CNE-2 or C666-1 xenografts. Darquet et al. (26) examined the activity of reporter genes 2 days after intratumoral transfection; however, the persistence of gene expression was not examined. In this study, we evaluated the persistence of transgene expression mediated by minicircle during 3 weeks after transfection. In the minicircle-treated group, IFNγ could be detected in tumors until 21 days after transfection, compared with 7 days in the p2ΦC31-IFNγ group. However, there was a progressive time-dependent reduction of IFNγ levels even in the minicircle group.

In contrast to our observations, Chen et al. (28) reported that animals infused with minicircle-huFIX expressed a high level of human FIX serum that was maintained for up to 7 weeks. The main difference between their report and ours is the host cell (hepatocytes versus tumor cells). The persistence of transgene expression from the minicircle can be achieved in cells with a low cell turnover rate, such as hepatocyte and skeletal muscle cell (28). In our study, most of the transfected cells were tumor cells with a doubling time of 1 to 3 days. Either cell division during the treatment or cell death caused by IFNγ will result in dilution of the nonreplicative minicircle vector and loss of transgene expression. The time-dependent reduction of IFNγ levels was also observed in minicircle-IFNγ–transfected C666-1 cells on day 6 (Fig. 2C). In addition to the dilution of the vector, the shorter persistence seen in our study could be due to the slowing down of the cell machinery resulting from IFNγ treatment and the protease degradation in the culture medium (35). Although the persistence of transgene expression mediated by the minicircle in tumor tissue was not comparable to that achieved in liver tissue, the minicircle presents great potential in antitumor gene therapy, which is superior to conventional plasmid gene therapy and recombinant protein therapy.

IFNγ gene therapy has not been applied to NPC. Our study reveals that IFNγ gene transfer mediated by the minicircle vector is a promising novel approach for treatment of NPC. Further studies of the mechanism governing the effects of IFNγ on the regulation of cell cycle arrest and apoptosis will be important for measuring its therapeutic potential and for determining the optimal conditions of minicircle-IFNγ treatment for single or adjuvant therapy of human NPC.

Acknowledgments

We thank Dr. Zhiying Chen (Stanford University, Stanford, CA) for his generous gift of p2ΦC31 and advice on this work; Dr. Qiang Liu (Sun Yat-sen University, Guangzhou, PR China) for critical reading of the manuscript and comments; and Miss Yingjun Ji and Han Liu (Sun Yat-sen University, Guangzhou, PR China) for helpful discussions and technical assistance.

References

1. Pang KR, Wu JJ, Huang DB, Tyring SK, Baron S. Biological and clinical basis for molecular studies of interferons. Methods Mol Med 2005;116:1–23.
2. Liu M, Acres B, Balloul JM, et al. Gene-based vaccines and immunotherapeutics. Proc Natl Acad Sci U S A 2004;101 Suppl:14567–71.
3. Chada S, Ramesh R, Mhashilkar AM. Cytokine- and chemokine-based gene therapy for cancer. Curr Opin Mol Ther 2003;5:463–74.
4. Ferrantini M, Belardelli F. Gene therapy of cancer with interferon: lessons from tumor models and perspectives for clinical applications. Semin Cancer Biol 2000;10:145–57.
5. Gutterman JU. Cytokine therapeutics: lessons from interferon α. Proc Natl Acad Sci U S A 1994;91:1198–205.
6. Sangfelt O, Erickson S, Grander D. Mechanisms of interferon-induced cell cycle arrest. Front Biosci 2000;5:D479–87.
7. Chawla-Sarkar M, Lindner DJ, Liu YF, et al. Apoptosis and interferons: role of interferon-stimulated genes as mediators of apoptosis. Apoptosis 2003;8:237–49.
8. Detjen KM, Farwig K, Welzel M, Wiedenmann B, Rosewicz S. Interferon γ inhibits growth of human pancreatic carcinoma cells via caspase-1 dependent induction of apoptosis. Gut 2001;49:251–62.
9. Hobeika AC, Etienne W, Cruz PE, Subramaniam PS, Johnson HM. IFNγ induction of p21WAF1 in prostate cancer cells: role in cell cycle, alteration of phenotype and invasive potential. Int J Cancer 1998;77:138–45.
10. Shyu RY, Su HL, Yu JC, Jiang SY. Direct growth suppressive activity of interferon-α and -γ on human gastric cancer cells. J Surg Oncol 2000;75:122–30.
11. Yano T, Sugio K, Yamazaki K, et al. Direct IFN influence of interferon-γ on proliferation and cell-surface antigen expression of non-small cell lung cancer cells. Lung Cancer 2000;30:169–74.
12. Cullinan AE, Brandt CR. Cytokine induced apoptosis in human retinoblastoma cells. Mol Vis 2004;10:315–22.
13. Hillman GG, Slos P, Wang Y, et al. Tumor irradiation followed by intratumoral cytokine gene therapy for murine renal adenocarcinoma. Cancer Gene Ther 2004;11:61–72.
14. Hopfner M, Sutter AP, Huether A, Ahnert-Hilger G, Scherubl H. A novel approach in the treatment of neuroendocrine gastrointestinal tumors: additive antiproliferative effects of interferon-γ and meta-iodobenzylguanidine. BMC Cancer 2004;4:23.
15. Gollob JA, Sciambi CJ, Huang Z, Dressman HK. Gene expression changes and signaling events associated with the direct antimelanoma effect of IFN-γ. Cancer Res 2005;65:8869–77.
16. Lugovic L, Situm M, Kos L. Malignant melanoma—future prospects. Acta Dermatovenerol Croat 2005;13:36–43.

17. Chan AT, Teo PM, Huang DP. Pathogenesis and treatment of nasopharyngeal carcinoma. Semin Oncol 2004;31:794–801.

18. Spano JP, Busson P, Atlan D, et al. Nasopharyngeal carcinomas: an update. Eur J Cancer 2003;39:2121–35.

19. Young LS, Murray PG. Epstein-Barr virus and oncogenesis: from latent genes to tumours. Oncogene 2003;22:5108–21.

20. Wakisaka N, Pagano JS. Epstein-Barr virus induces invasion and metastasis factors. Anticancer Res 2003; 23:2133–8.

21. Weinrib L, Li JH, Donovan J, Huang D, Liu FF. Cisplatin chemotherapy plus adenoviral p53 gene therapy in EBV-positive and -negative nasopharyngeal carcinoma. Cancer Gene Ther 2001;8:352–60.

22. Li JH, Lax SA, Kim J, Klamut H, Liu FF. The effects of combining ionizing radiation and adenoviral p53 therapy in nasopharyngeal carcinoma. Int J Radiat Oncol Biol Phys 1999;43:607–16.

23. Li JH, Shi W, Chia M, et al. Efficacy of targeted FasL in nasopharyngeal carcinoma. Mol Ther 2003;8: 964–73.

24. Cheung ST, Huang DP, Hui AB, et al. Nasopharyngeal carcinoma cell line (C666–1) consistently harbouring Epstein-Barr virus. Int J Cancer 1999;83: 121–6.

25. Darquet AM, Cameron B, Wils P, Scherman D, Crouzet J. A new DNA vehicle for nonviral gene delivery: supercoiled minicircle. Gene Ther 1997;4:1341–9.

26. Darquet AM, Rangara R, Kreiss P, et al. Minicircle: an improved DNA molecule for *in vitro* and *in vivo* gene transfer. Gene Ther 1999;6:209–18.

27. Bigger BW, Tolmachov O, Collombet JM, Fragkos M, Palaszewski I, Coutelle C. An araC-controlled bacterial cre expression system to produce DNA minicircle vectors for nuclear and mitochondrial gene therapy. J Biol Chem 2001;276:23018–27.

28. Chen ZY, He CY, Ehrhardt A, Kay MA. Minicircle DNA vectors devoid of bacterial DNA result in persistent and high-level transgene expression *in vivo*. Mol Ther 2003;8:495–500.

29. Chen ZY, He CY, Meuse L, Kay MA. Silencing of episomal transgene expression by plasmid bacterial DNA elements *in vivo*. Gene Ther 2004;11:856–64.

30. Chen ZY, He CY, Kay MA. Improved production and purification of minicircle DNA vector free of plasmid bacterial sequences and capable of persistent transgene expression *in vivo*. Hum Gene Ther 2005;16: 126–31.

31. Ahmed CM, Burkhart MA, Subramaniam PS, Mujtaba MG, Johnson HM. Peptide mimetics of γ interferon possess antiviral properties against vaccinia virus and other viruses in the presence of poxvirus B8R protein. J Virol 2005;79:5632–9.

32. Sakon S, Xue X, Takekawa M, et al. NF-κB inhibits TNF-induced accumulation of ROS that mediate prolonged MAPK activation and necrotic cell death. EMBO J 2003;22:3898–909.

33. Khorana AA, Rosenblatt JD, Sahasrabudhe DM, et al. A phase I trial of immunotherapy with intratumoral adenovirus-interferon-γ (TG1041) in patients with malignant melanoma. Cancer Gene Ther 2003; 10:251–9.

34. Nowak AK, Lake RA, Kindler HL, Robinson BW. New approaches for mesothelioma: biologics, vaccines, gene therapy, and other novel agents. Semin Oncol 2002;29:82–96.

35. Gattacceca F, Pilatte Y, Billard C, et al. Ad-IFNγ induces antiproliferative and antitumoral responses in malignant mesothelioma. Clin Cancer Res 2002;8: 3298–304.

36. Cordier KL, Valeyrie L, Fernandez N, et al. Regression of AK7 malignant mesothelioma established in immunocompetent mice following intratumoral gene transfer of interferon γ. Cancer Gene Ther 2003;10: 481–90.

37. Dummer R, Hassel JC, Fellenberg F, et al. Adenovirus-mediated intralesional interferon-γ gene transfer induces tumor regressions in cutaneous lymphomas. Blood 2004;104:1631–8.

38. Wu CM, Li XY, Huang TH. Anti-tumor effect of pEgr-IFNγ gene-radiotherapy in B16 melanoma-bearing mice. World J Gastroenterol 2004;10:3011–5.

39. Burke F, East N, Upton C, Patel K, Balkwill FR. Interferon γ induces cell cycle arrest and apoptosis in a model of ovarian cancer: enhancement of effect by batimastat. Eur J Cancer 1997;33:1114–21.

40. Burke F, Smith PD, Crompton MR, Upton C, Balkwill FR. Cytotoxic response of ovarian cancer cell lines to IFN-γ is associated with sustained induction of IRF-1 and p21 mRNA. Br J Cancer 1999;80: 1236–44.

41. Kim EJ, Lee JM, Namkoong SE, Um SJ, Park JS. Interferon regulatory factor-1 mediates interferon-γ-induced apoptosis in ovarian carcinoma cells. J Cell Biochem 2002;85:369–80.

42. Wall L, Burke F, Barton C, Smyth J, Balkwill F. IFN-γ induces apoptosis in ovarian cancer cells *in vivo* and *in vitro*. Clin Cancer Res 2003;9:2487–96.

43. Barton C, Davies D, Balkwill F, Burke F. Involvement of both intrinsic and extrinsic pathways in IFN-γ-induced apoptosis that are enhanced with cisplatin. Eur J Cancer 2005;41:1474–86.

44. Ruiz-Ruiz C, Ruiz de Almodovar C, Rodriguez A, Ortiz-Ferron G, Redondo JM, Lopez-Rivas A. The up-regulation of human caspase-8 by interferon-γ in breast tumor cells requires the induction and action of the transcription factor interferon regulatory factor-1. J Biol Chem 2004;279:19712–20.

45. Tomita Y, Bilim V, Hara N, Kasahara T, Takahashi K. Role of IRF-1 and caspase-7 in IFN-γ enhancement of Fas-mediated apoptosis in ACHN renal cell carcinoma cells. Int J Cancer 2003;104:400–8.

46. Merchant MS, Yang X, Melchionda F, et al. Interferon γ enhances the effectiveness of tumor necrosis factor-related apoptosis-inducing ligand receptor agonists in a xenograft model of Ewing's sarcoma. Cancer Res 2004;64:8349–56.

47. Papageorgiou A, Lashinger L, Millikan R, et al. Role of tumor necrosis factor-related apoptosis-inducing ligand in interferon-induced apoptosis in human bladder cancer cells. Cancer Res 2004;64:8973–9.

48. Ruiz-Ruiz C, Munoz-Pinedo C, Lopez-Rivas A. Interferon-γ treatment elevates caspase-8 expression and sensitizes human breast tumor cells to a death receptor-induced mitochondria-operated apoptotic program. Cancer Res 2000;60:5673–80.

49. Farber JM. Mig and IP-10: CXC chemokines that target lymphocytes. J Leukoc Biol 1997;61:246–57.

50. Sgadari C, Angiolillo AL, Tostato G. Inhibition of angiogenesis by interleukin-12 is mediated by the interferon-inducible protein-10. Blood 1996;87:3877–81.

Clinical Cancer Research

Minicircle-IFNγ Induces Antiproliferative and Antitumoral Effects in Human Nasopharyngeal Carcinoma

Jiangxue Wu, Xia Xiao, Peng Zhao, et al.

Clin Cancer Res 2006;12:4702-4713.